

*Original Article*

# Geochemical indices and palynology comparison used for paleoproductivity and paleoredox conditions of the Huai Hin Lat Formation in part of Loei-Petchabun Fold Belt in central Thailand

Boonnarong Arsairai<sup>1\*</sup>, Qinglai Feng<sup>2</sup>, Chongpan Chonglakmani<sup>1</sup>,  
Akkhapun Wannakomol<sup>1</sup>, and Hathaichanok Vattanasak<sup>3</sup>

<sup>1</sup> School of Geotechnology, Institute of Engineering,  
Suranaree University of Technology, Mueang, Nakhon Ratchasima, 30000 Thailand

<sup>2</sup> State Key Laboratory of Geological Processes and Mineral Resources,  
China University of Geosciences, Wuhan, 430074 China

<sup>3</sup> Department of Mining and Materials Engineering, Faculty of Engineering,  
Prince of Songkla University, Hat Yai, Songkhla, 90110 Thailand

Received: 20 November 2018; Revised: 4 February 2019; Accepted: 10 March 2019

---

## Abstract

Petrography and geochemistry analyzing Dat Yai section can describe paleoproductivity and past-redox condition. Paleoproductivity proxies consisted of AOM, phytoclast, TOC, excess SiO<sub>2</sub>, Ba/Al, and P/Al as high values through sections which similarly indicate high productivity. High productivity in Beds 3 and 27 showed lower peak TOC which is explained by poorer preservation. Lower productivity of Bed 18 showed a high TOC peak indicating good preservation. Paleoredox condition was evaluated using Ni/Co, U/Th, V/Cr, V/(V+Ni), Ni/V, and (Cu+Mo)/Zn. Values for V/(V+Ni) ranged from 0.67 to 0.85 exceeding the cutoff value of 0.46 for a reducing environment. The average value of V/Cr (2.07) exceeded 2.0 of anoxic. Bed 9 consisted of the highest peak of TOC that does not reflect the excellent preservation resulting from dominantly high paleoproductivity. Bed 21 exhibited lower productivity and lowest TOC which indicated a poverty-reducing effect. AOM and phytoclasts were supplied and kept in the benthic floor by extreme redox. Sediments became black shale which expelled oil and some gas.

**Keywords:** TOC, hydrocarbon, geochemistry, kerogen, petrography, Huai Hin Lat Formation

---

## 1. Introduction

The Khorat Plateau is an energy-starved region with a large population providing a ready market for any gas. Despite past disappointments, this basin continues to attract exploration (Booth, 1998). Therefore, the Thai government lets international companies bid for petroleum exploration concessions to reduce the volume of imported petroleum. At

present, no wells show any significant amount of tested oil. Natural gas was discovered in three commercial gas fields of Nam Phong, Sin Phu Horm, and Dong Mun gas fields but gas was produced recently only in two former fields (D.M.F., 2014). However, national and international companies are also interested in this area as they expect to develop both conventional and unconventional natural gas, especially shale gas.

Source rock qualities of the Huai Hin Lat Formation were initially studied. Much geochemical data of Huai Hin Lat rocks containing a very good to fair source richness (Satta yarak, Srikulwong, & Pum-In, 1989; Chinoroje & Cole, 1995;

---

\*Corresponding author

Email address: rong\_geo@hotmail.com

Piyasin, 1995) were published on online. Maturation ranges from mature to very mature. Both gas and liquid hydrocarbons can be produced from organic matter (Satta yarak *et al.*, 1996). However, nobody has suggested any reason why the Huai Hin Lat Formation could provide essential petroleum potential in northeastern Thailand. One among other reasons, it may be associated with sedi-mentations of both organic matter supply and depositional conditions in the Huai Hin Lat basin as in a lake.

Changes in the mass and the sources of elemental compositions have affected the sediment geochemistry (Arsairai, Wannakomol, Feng, & Chonglakmani, 2016) of the lake basin as provided in high resolution paleoclimatic records (Johnson, Fawcett, & Ali, 2007). Moreover, the collected shale samples from the stratigraphic unit were analyzed on the basis of petrography and geochemistry to describe the paleo-productivity and the redox environment (Eusterhues, Heinrichs, & Schneider, 2005; Martin-Puertas *et al.*, 2011).

## 2. Measured Section of the Dat Yai

### 2.1 Tectonic setting and stratigraphy

The drilling well data and seismic interpretation have contributed to showing the Huai Hin Lat Formation distribution and expansion. There are three exposed basins and six subsurface basins scattered on the Khorat Plateau. They resulted from the collision and fusion of the Sibumasu (also called Shan-Thai) (Chonglakmani, 2011) and that of the Indochina in the Permian-Triassic. Then the lake developed and sediments were deposited in the basin. Three exposed basins cropped out along the rim of the Khorat Plateau and are connected to the Permian Basin. The largest basin is located in the southwestern area of the Khorat Plateau showing a better prospective basin for investigation in its potential petroliferous basin. It is the combination of two basins of the Sap

Phlu Basin and Chok Chai Basins in which the uppermost part (the post-rift sequences) possibly join together. Another large basin is exposed at the northwestern area at the rim of the Khorat Plateau. It is the Huai Hin Lat Formation of the Na Pho Song Basin which exposes in part the Loei-Petchabun Fold Belt. The Huai Hin Lat Formation consists of conglomerate, sandstone, fine-grained rocks, and volcanic rocks of Pho Hai Member, Sam Khaen Conglomerate Member, Dat Fa Member, Phu Hi Member, and I Mo Member (Chonglakmani, 2011; Chonglakmani & Sattayalak, 1978). The *Estheria* fauna, spores, and pollen which were discovered indicated the Late Triassic (Norian) age (Haile, 1973; Kobayashi, 1973).

### 2.2 Measured section of the Dat Yai

The Dat Yai section is a part of the Na Pho Song Basin (Figure 1) located at 47Q 796604 N and 1850718 E along the flow directions of the Dat Yai waterfall. It is among the areas of Phu Pha Man District, Khon Kaen Province and Nam Nao District, and Petchabun Province close to the Phu Pha Man National Park. While only source rock data have been previously studied, other geochemical data have not been investigated. The section (Figure 2) is formed as the Lowest Na Pho Song Basin as these rocks are deposited in the deep lake basin with high preservation of organic matter and sediment supply. It is 42 m thick and is chiefly composed of calcareous fine-grained rocks. According to Chonglakmani and Sattayarak (1978), it can be correlated to deep lacustrine facies and the Na Pho Song Basin that is similar to the Ban Nong Sai section (Arsairai, Wannakomol, Feng, & Chonglakmani, 2016). The rocks with mostly a dull texture are greyish black to dark black. The argillaceous limestone is very resistant with a massive bed. In addition, the rock matrix appears to be calcite crystals dispersed through their beds of about 0.5–1 cm. The calcareous shale forms a thin bed of

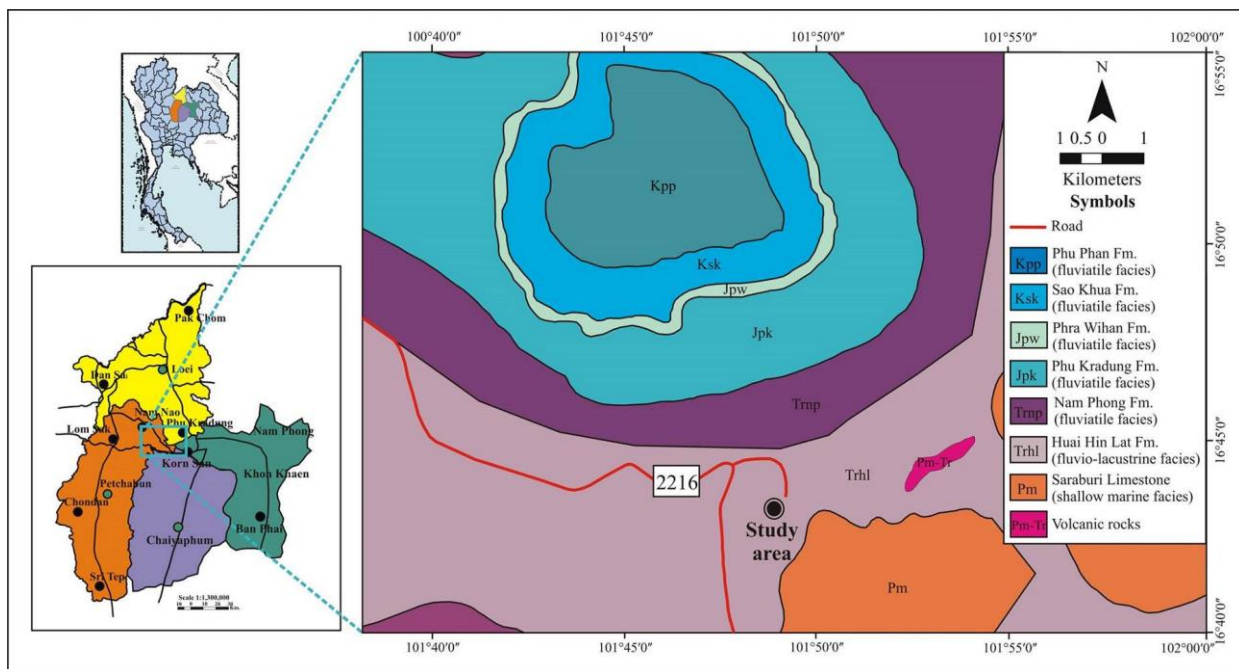


Figure 1. Geologic map showing location of the Dat Yai section.

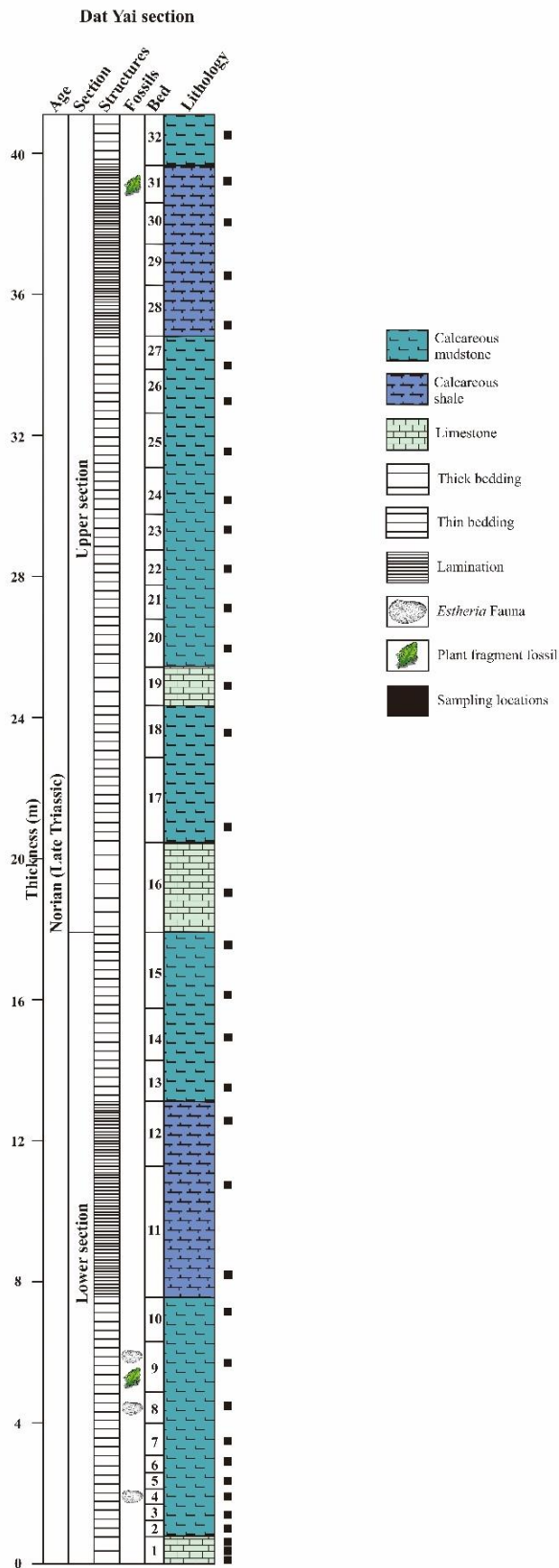


Figure 2. Lithologic column of the Dat Yai section (Na Pho Song Basin).

unclear fossil fuel reserves with 2–5 cm thickness but the calcareous mudstones are thicker. They are associated with slightly dispersed calcite crystals and are formed as layers in some parts of fine-grained rock matrix. These layered calcite crystals are a few millimeters to 1 cm thick. Lastly, two parts of the lower and the upper parts are subdivided.

The lower part (Beds 1–15) has more abundant bedding planes than the upper part and the dissolved calcite traces along their beds are observed. In addition, pyrites were found as unshaped bulbs and weathered pyrite showing a yellowish brown color similar to clay nodules. These pyrites are more dispersed and abundant through their beds, especially in the upper part (Beds 16–32). Plant fragments are more abundant in the upper part of beds 9 and 31 but cannot be identified according to the maceral group due to poor preservation. Moreover, the common fossils of *Estheria* sp. are abundant in beds 4, 8, and 9. They are identified as belonging to the Norian age following the reasons and suggestions of Kobayashi (1973). These plant fragments and *Estheria* sp. that accumulated as organic matter can generate hydrocarbons for petroleum systems. Forces have affected this section by bedding joints with bedding attitudes of 208/82 and 343/88 on bed 10, 335/68, 014/89, and 114/66 on bed 19, and 251/85, and 333/88 on bed 16. D.M.R. (2012) studied thin sections of black earth minerals in the Dat Yai waterfall and found interesting structures. They suggested that diagenetic processes have affected this measured stratigraphic section. The diagenetic processes generated the stylolitic structures forming saw teeth styles. This was discovered along the dissolved bed due to the influence of pressure solution (D.M.R., 2012).

### 3. Materials and Methods

Lithologic section measurement and sedimentologic characteristics were described based on rocks cropping out. Unweathered samples were collected from the studied section to assess the source rock potential. The palynological assemblages were defined as proxies using rock extraction of petrographic studies. Consequently, total organic carbon (TOC) content and other elements including major elements, trace elements, and rare earth elements (REEs) were identified and also established as proxies using a geochemical analysis study.

#### 3.1 Petrographic analysis

The standard palynological method was used for a petrographic study following Albani *et al.* (2006) of spiking with a known number of lycopodium spores. The residue samples were observed by light microscopy to count the frequency ratio of amorphous organic matter (AOM), palynomorphs, and phytoclasts to lycopodium spores (Arsairai, Wannakomol, Feng, & Chonglakmani, 2016).

#### 3.2 Geochemical analysis

The TOC content was carried out using a Liqui TOC instrument ( $\pm 1\%$  error) at the State Key Laboratory of Biogeology and Environmental Geology of the Ministry of Education, China University of Geosciences (Wuhan). Fused glass beads with a XRF-1800 instrument ( $\pm 10\%$  error) based

on wavelength-dispersive X-ray fluorescence (XRF) was used to analyze the major elements at the State Key Laboratory of Geological Processes and Mineral Resources. Inductively coupled plasma mass spectrometry ( $\pm 5\%$  error) was used to measure the trace elements and REEs at the State Key Laboratory of Biology and Environmental Geology of the Ministry of Education. Both laboratories are parts of the China University of Geosciences (Wuhan).

#### 4. Results

For more comprehensibility, the accumulation and organic matter preservation were kept in the formation. The paleoproductivity and paleoredox were the key control conditions carried out by petrographic and geochemical analysis.

##### 4.1 Petrographic analysis

The petrographic analysis of the Dat Yai samples showed a high amount of palynology by the point-count method. The point-count results of cumulative percentages are

shown in Table 1, Figures 3 and 5a consist of AOM, palynomorphs, phytoclasts, and spores and pollen (lack of diversity).

AOM concentrations (Figures 3c and 4b) showed relatively high fluctuations throughout the section (Figure 4b). It illustrated occasional clustering blooms of AOM with values ranging from 8,794 to 967,019 particles/g of rock and 378,182 particles/g of rock of a moderate value. They were generally higher than other palynofacies. The lowest section was low and gradually increased upward to the upper lower section with 374,302 particles/g of rock of an average value. The trend showed six high peaks in the lower part in Beds 5, 8, 11, 12, 13, and 14 with values of 687,747, 603,592, 553,477, 576,646, 620,727, and 967,019 particles/g of rock, respectively. The concentrations in the upper part were as high due to increasing upward to Bed 22 and decreasing upward to the uppermost. The trend showed four high peaks in Beds 18, 22, 27, and 30 with values of 513,274, 815,070, 559,152, and 472,777 particles/g of rock, respectively, that corresponded with the trend of AOM.

Table 1. Palynofacies point count (particles/g) and TOC content data.

Bed	Palynofacies point count (Particles/g of rock)			Palynofacies fraction (Cumulative percentage)			TOC (%)
	AOM	Phytoclasts	Palynom.	AOM	Phytoclasts	Palynom.	
32	194,749	1,525,532	0.00	11.32	88.68	0.00	7.79
31	413,450	856,431	0.00	32.56	67.44	0.00	7.78
30	472,777	118,194	0.00	80.00	20.00	0.00	8.09
29	252,971	233,511	0.00	52.00	48.00	0.00	8.10
28	489,797	827,990	0.00	37.17	62.83	0.00	5.76
27	559,152	1,118,304	0.00	33.33	66.67	0.00	5.77
26	319,760	75,238	0.00	80.95	19.05	0.00	6.78
25	113,589	2,214,967	0.00	4.88	95.12	0.00	6.93
24	393,709	64,018	0.00	86.01	13.99	0.00	6.13
23	462,975	89,608	0.00	83.78	16.22	0.00	6.19
22	815,070	140,876	0.00	85.26	14.74	0.00	6.13
21	416,351	45,538	0.00	90.14	9.86	0.00	4.67
20	308,540	71,201	0.00	81.25	18.75	0.00	5.59
19	340,267	61,867	0.00	84.62	15.38	0.00	6.00
18	513,274	85,546	0.00	85.71	14.29	0.00	7.46
17	282,727	55,924	0.00	83.49	16.51	0.00	6.52
16	157,531	866,420	0.00	15.38	84.62	0.00	8.08
15	315,860	38,520	0.00	89.13	10.87	0.00	7.23
14	967,019	153,191	0.00	86.32	13.68	0.00	7.37
13	620,727	64,659	0.00	90.57	9.43	0.00	5.99
12	576,646	48,054	0.00	92.31	7.69	0.00	7.42
11_2	121,879	52,234	0.00	70.00	30.00	0.00	7.53
11_1	553,477	113,534	0.00	82.98	17.02	0.00	7.70
10	221,950	31,707	0.00	87.50	12.50	0.00	6.74
9	477,457	44,937	0.00	91.40	8.60	0.00	10.09
8	603,592	71,011	0.00	89.47	10.53	0.00	8.17
7	65,971	9,425	0.00	87.50	12.50	0.00	8.17
6	387,913	31,283	0.00	92.54	7.46	0.00	-
5	687,747	114,625	0.00	85.71	14.29	0.00	6.74
4	304,698	39,743	0.00	88.46	11.54	0.00	-
3	203,316	23,460	0.00	89.66	10.34	0.00	6.30
2	203,760	29,885	0.00	87.21	12.79	0.00	-
1_3	135,854	13,863	0.00	90.74	9.26	0.00	6.84
1_2	53,558	6,301	0.00	89.47	10.53	0.00	-
1_1	8,794	799	0.00	91.67	8.33	0.00	-

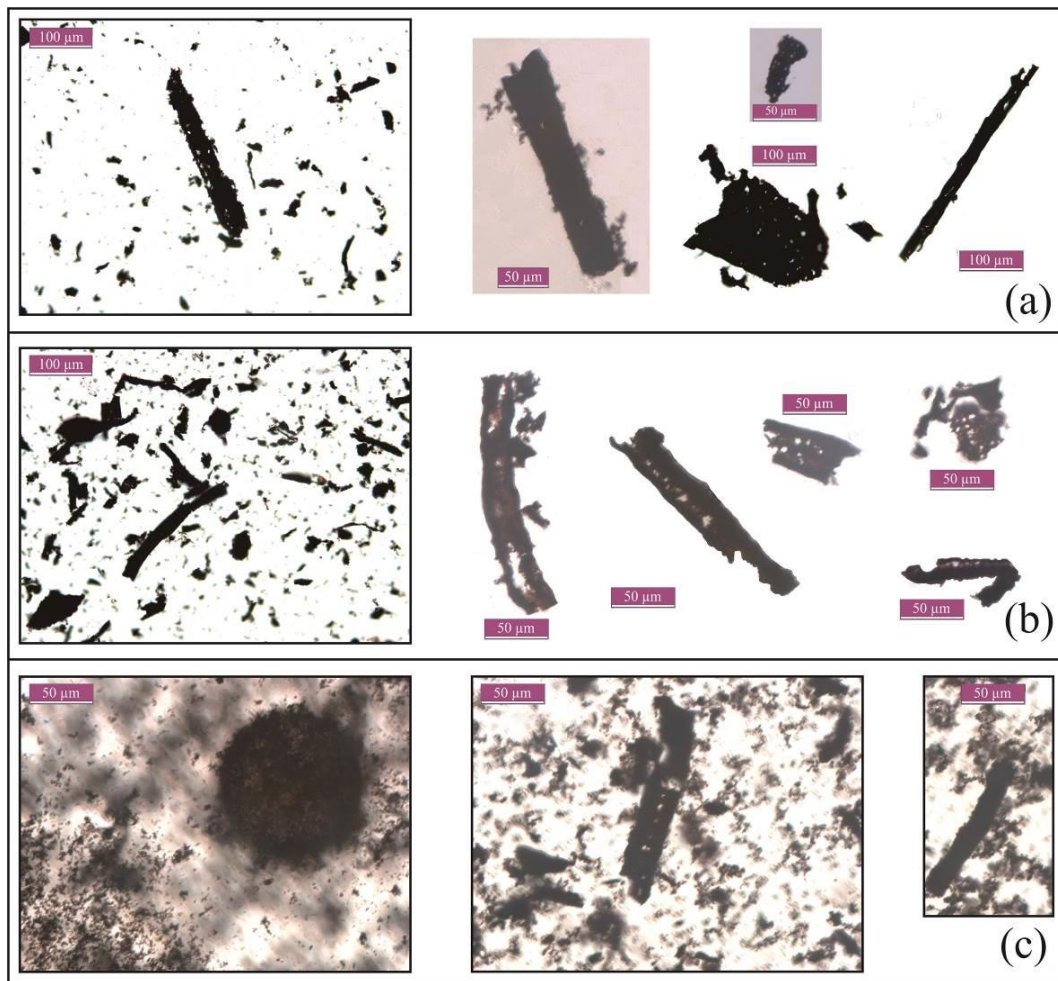


Figure 3. Photomicrographs of particulate organic components of selected samples under transmitted light: (a) Opaque biostructured phytoclasts; (b) Non-opaque biostructured phytoclasts; (c) Phytoclasts and AOM.

Phytoclast concentration was identified as two types of opaque and non-opaque biostructures. The opaque and non-opaque biostructured phytoclasts were pitted and elongated shapes of fragments (Figures 3a–3b). Their concentrations showed relative fluctuations throughout the section (Figure 4c). They showed values ranging from 799 to 2,214,967 particles/g of rock and stabilized at an average value of 312,275 particles/g of rock. The lower section had low concentrations of an average value of 52,061 particles/g of rock. It had four high peaks in Beds 5, 8, 11, and 14 with values of 114,624, 71,011, 113,534, and 153,191 particles/g of rock, respectively. The upper part showed higher values ranging from 45,538 to 2,214,967 and the average value of 563,772 particles/g of rock. The trend increased by seven high peaks in Beds 16, 22, 25, 27, 28, 31, and 32 with values of 866,420, 140,876, 2,214,967, 1,118,304, and 1,525,532 particles/g of rock, respectively.

Spore and pollen concentrations were not discovered throughout the section due to the position of the lake. They were significantly found at the rim of the lake area or near the shore of the lake depending on land sources. According to the Dat Yai section, it indicated deep lacustrine sediments following Chonglakmani and Sattayarak (1978)

which were far away from palynomorph sources. Therefore, it showed that the deposit did not foster the settling down of palynomorphs.

Acritarch concentrations were not discovered throughout the section which was similar to spores and pollen. Although they should be abundant in deep lacustrine, they were lacking. However, due to the high relationship with AOM, they probably changed to AOM depending on degradation effects.

The organic matter consisted mainly of AOM belong to only type I kerogen and some phytoclasts of type III kerogen; therefore, oil and some gas expelled to the Na Pho Song Basin. Moreover, oil cracked to gas at higher volumes that caused higher thermal maturity level ( $R_o$ ).

## 4.2 Geochemical analysis

### 4.2.1 Total organic carbon (TOC) content

The values of the TOC content proxies ranged from 4.67% to 10.09% with an average value of 7.03% which indicated high productivity, especially in the lower section (Figure 4d). The trend was high (6.84%) at the basal part with

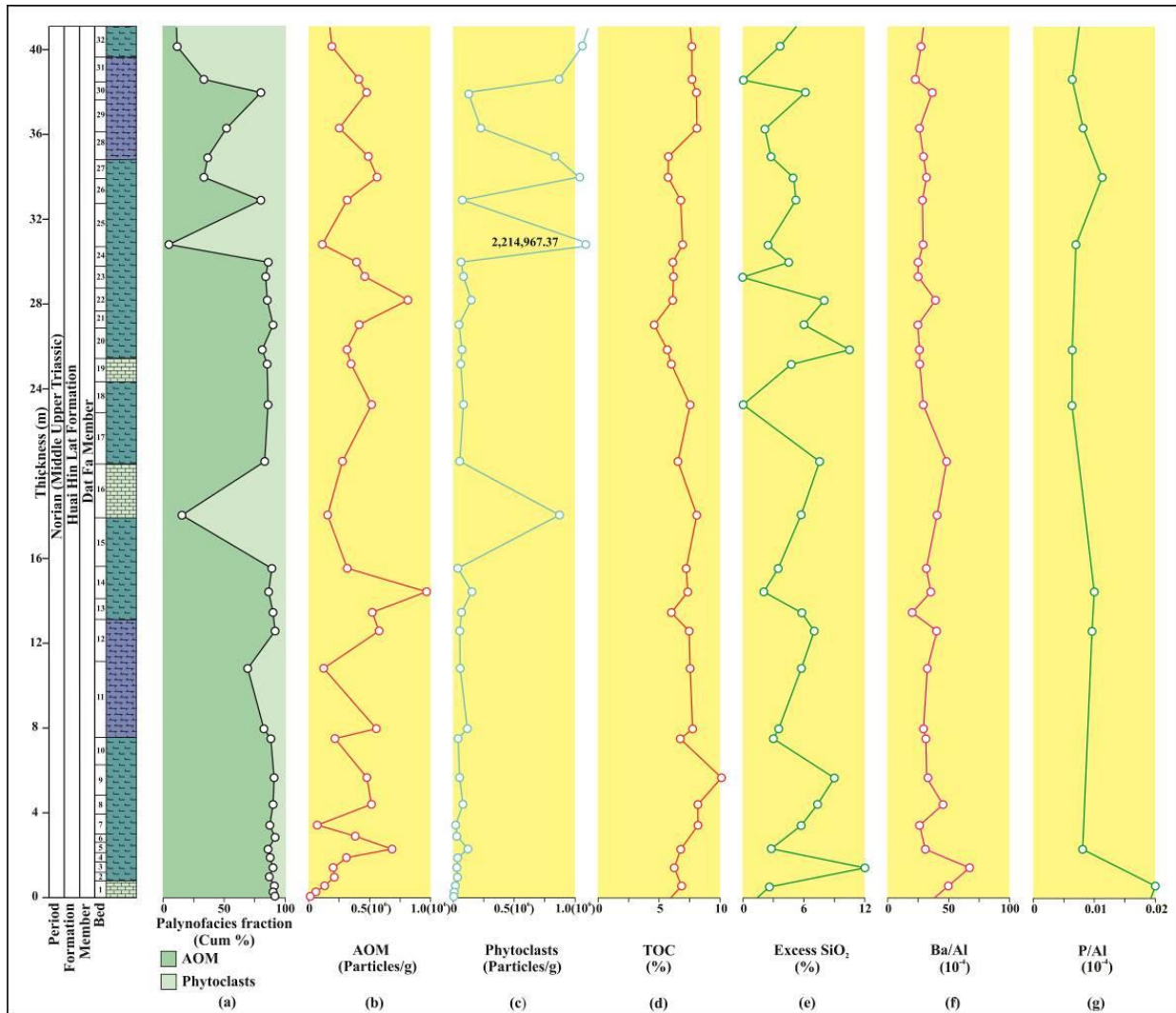


Figure 4. Bio- and chemostratigraphic data: (a) Palynofacies (AOM, and phytoclast) fraction; (b) AOM; (c) Phytoclast abundance; (d) Total organic carbon (TOC); (e) The normalized Ba/Al trend; and (f) The normalized P/Al trend.

an average value of 7.49%. It increased upward to Bed 9 and constantly declined upward to the upper part. It showed peaks of Beds 1, 9, 11, 12, and 14 with the values of 6.84, 10.09, 7.70, 7.42, and 7.37%, respectively. It moderately corresponded with the peaks of AOM and phytoclasts. Then it slightly declined to Bed 20 and increased upward to the uppermost with an average of 6.66%. The six high peaks of the Beds 16, 18, 25, 26, 29, and 30 were 8.08, 7.46, 6.93, 6.78, 8.10, and 8.09, respectively, but did not correspond with the acritarchs and phytoclasts peaks.

#### 4.2.2 Excess SiO<sub>2</sub>

The values of excess silica ranged from a very low value up to 11.99% with an average value of 4.89% (Figure 4e) that was mainly derived from hard parts of diatoms. They were the highest in the basal part and gradually declined to the upper lower section that averaged 5.62%. The three high peaks were in Beds 3, 9, and 12 with values of 11.99, 9.00, and 7.04%, respectively. The upper section showed values

that ranged up to 10.40% and relatively low to an average value of 4.46%. Then the eight high peaks were shown in Beds 17, 20, 22, 24, 26, 27, 30, and 32 with values of 7.48, 10.40, 8.03, 4.45, 5.15, 4.89, 6.13, and 3.69%, respectively.

#### 4.2.3 Normalized Ba/Al

The Ba/Al ratio ranged from 19.90 ( $10^{-4}$ ) to 67.39 ( $10^{-4}$ ) with an average value of 33.41 ( $10^{-4}$ ) (Figure 4f). The lower section showed the highest peak of Bed 3 with an average value of 37.20 ( $10^{-4}$ ). Other high peaks still appeared in Beds 8, 12, and 14 with values of 44.75 ( $10^{-4}$ ), 40.40 ( $10^{-4}$ ), and 35.37 ( $10^{-4}$ ), respectively. They corresponded with the trend of excess SiO<sub>2</sub>, phytoclasts, and AOM. The upper section showed high peaks of Beds 17, 22, 27, and 30 with values of 47.67 ( $10^{-4}$ ), 38.93 ( $10^{-4}$ ), 31.88 ( $10^{-4}$ ), and 35.81 ( $10^{-4}$ ), respectively. The pattern still conformed with the AOM, phytoclasts, and excess silica peaks. The trend then slightly declined to the uppermost section showing a value of 30.62 ( $10^{-4}$ ) which was a slightly low average.

**4.2.4 Normalized P/Al**

The normalized P/Al ranged from 0.0061 ( $10^{-4}$ ) to 0.0217 ( $10^{-4}$ ) with an average of 0.0091 ( $10^{-4}$ ) (Figure 4g). The lower section showed three high peaks with an average value of 0.0131 ( $10^{-4}$ ) which corresponded with the others except the peak of the basal part which corresponded only with TOC. Bed 1 had the highest peak and the values of both Beds 12 and 14 were 0.0094 ( $10^{-4}$ ) and 0.0099 ( $10^{-4}$ ), respectively. The trend then increased upward to Bed 27 which was 0.0084 ( $10^{-4}$ ) and slightly declined in the uppermost section with an average value of 0.0071 ( $10^{-4}$ ).

**4.2.5 Ni/Co relationship**

The trend's fluctuations (Figure 5a) are shown as ratios of Ni/Co that varied between 0.62 and 1.17 with an average value of 0.65. For the lower part, they maintained a normal level in the range of 0.62–1.07 and stabilized at an

average value of 0.91. It showed three high peaks of Beds 5, 10, 11, and 12 with the values of 1.02, 1.07, and 1.07, respectively. In the upper part, the trend slightly rose with values ranging from 0.71 to 1.17 with an average of 0.97. It showed seven high peaks of Beds 16, 17, 19, 20, 24, 27, and 32 with values of 1.15, 1.04, 1.05, 1.15, 1.09, 1.19, and 1.16, respectively.

**4.2.6 U/Th relationship**

Values of the U/Th ratio are shown in Figure 5b and present relatively high fluctuations throughout the section. The ratio was a high average value of 0.51 and ranged from around 0.74 to around 0.36 with occasional declinations. The average ratio of the lower section was 0.49 which showed high values at the basal part with occasional declines. The lower trend showed four high peaks of Beds 5, 8, 10, and 13 with the values of 0.74, 0.57, 0.48, and 0.45, respectively. The upper part constantly increased to approximately 0.38–0.68

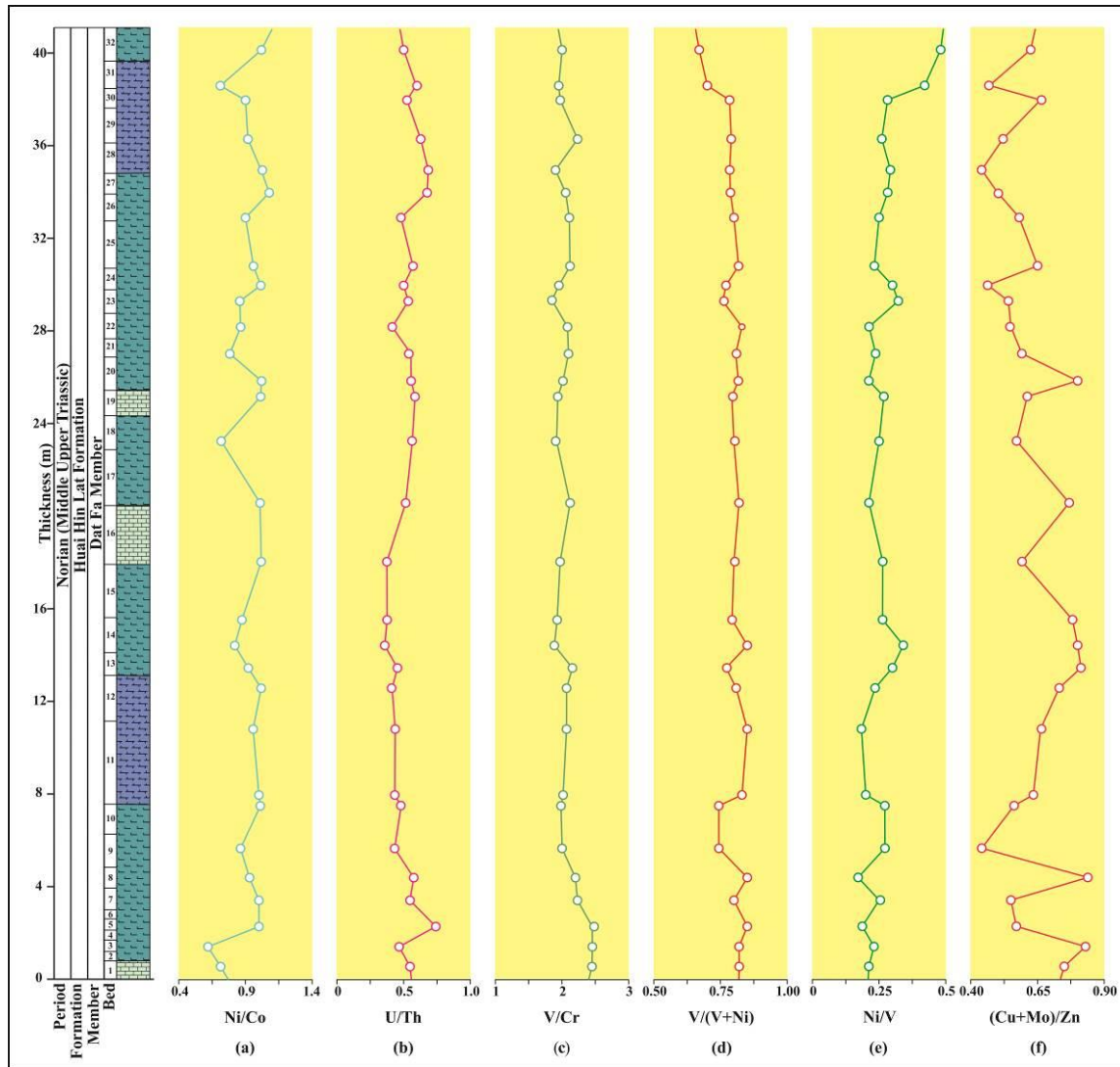


Figure 5. Chemostratigraphic data: (a) U/Th relationship; (b) U/Th relationship; (c) V/Cr relationship; (d) V/(V+Ni) relationship; (e) Ni/V relationship; (f) (Cu+Mo)/Zn relationship.

with an average of 0.54. It showed relatively high values of 0.58, 0.53, 0.57, and 0.67 of Beds 19, 23, 25, and 27, respectively.

#### 4.2.7 V/Cr relationship

The value of the V/Cr relationship fluctuated and varied between 1.84 and 2.46 with 2.07 as the average (Figure 5c). The value of the lowermost section was high and slightly declined upward. Substantial variations ranged from 1.87 to 2.46 with an average of 2.8. They showed four high peaks of Beds 5, 8, 11, and 13 with values of 2.44, 2.20, 2.02, and 2.15, respectively. These peaks relatively corresponded with the Ni/Co and U/Th trends. In the upper section, the trend slightly increased upward with values at around 1.84–2.22 with an average value of 2.01. There were four high peaks of Beds 17, 21–22, 25, and 29 with the values of 2.12, 2.07, 2.10, and 2.22, respectively. They slightly corresponded with the trends of Ni/Co and U/Th; however, some parts still exhibited similar patterns.

#### 4.2.8 V/(V+Ni) relationship

The ratio of V/(V+Ni) was high throughout the section which ranged from 0.67 to 0.85 and stabilized at an average value of 0.79 (Figure 5d). The lower section increased to 0.75–0.85 with an average of 0.81. It showed four high peaks of Beds 5, 8, 11, and 14 with values of 0.85, 0.85, 0.83, and 0.75 respectively. These peaks corresponded with the high peak of Ni/Co and U/Th. The ratios declined to 0.67–0.83 with an average of 0.78 in the upper part and suddenly declined in the uppermost part. It showed five peaks of Beds 17, 21, 22, 25, and 29 that corresponded with the V/Cr trend.

#### 4.2.9 Ni/V relationship

The values of the Ni/V relationship of the Dat Yai section ranged from 0.17–0.48 with 0.27 as the average (Figure 5e). The lowermost section was low and slightly increased upward with the values ranging from 0.17 to 0.34 with 0.24 as the average. It showed high Ni/V ratios of 0.23, 0.25, 0.27, and 0.34 in Beds 3, 7, 9, 10, and 14, respectively. In the upper section, the values still rose to the uppermost section that was around 0.21–0.48 with an average value of 0.29. The high values of 0.27 and 0.32 were shown in Beds 19, 23, especially Bed 32 was the highest. All high peaks (high values) exhibited patterns which significantly contrasted with the patterns of V/Cr and V/(V+Ni).

#### 4.2.10 (Cu+Mo)/Zn relationship

The values of the (Cu+Mo)/Zn relationship ranged from 0.44 to 0.84 with an average value of 0.63 (Figure 5f). They fluctuated through the section where the lower part had a high value at the base, declined upward to Bed 9, and increased upward to Bed 13. The values of the lower section varied between 0.44 and 0.84 with an average value of 0.68. Beds 3 and 8 showed high values of 0.83 and 0.84, respectively. The trend generally declined upward to the uppermost section with values of around 0.44–0.80 with 0.59 as the average. Four high peaks were shown in Beds 17, 20, 25, and 30 with values of 0.77, 0.80, 0.65, and 0.66,

respectively. They exhibited a few peaks which corresponded with the high peaks of the other proxies.

## 5. Discussion

The paleoproductivity and the reducing events of the benthic floor of the basin can be assessed using the obtained petrographic and geochemical results.

### 5.1 Lacustrine paleoproductivity

In the section that was studied, the high peaks or high concentrations can be related to high productivity of the measured section.

The lower section showed four high peaks that appeared in Beds 3, 9, 12, and 14. The sharp peak of Bed 3 was consistent with the excess SiO<sub>2</sub>, Ba/Al, and P/Al (still high). The sharp peak of Bed 9 corresponded with AOM and excess SiO<sub>2</sub>. Moreover, the sharp peaks of Beds 12 and 14 corresponded with phytoclasts, AOM, excess SiO<sub>2</sub>, Ba/Al, and P/Al. They may be used to indicate high productivity where it shows. These high peaks may also be used to indicate the lowest productivity.

The upper section showed six high peaks in Beds 16, 17, 22, 27, 30, and 32 that were distributed throughout their parts. The high peaks of Beds 16 and 17 conformed to AOM, phytoclasts, excess SiO<sub>2</sub>, and Ba/Al. Bed 16 showed an unclear peak of excess SiO<sub>2</sub> and Ba/Al; however, they still exhibited high values. The high peaks of Beds 22 and 27 corresponded with AOM, phytoclasts, excess SiO<sub>2</sub>, Ba/Al, and P/Al. The high peak of Bed 30 supported conformity with AOM, excess SiO<sub>2</sub>, and Ba/Al. The high concentration of Bed 32 conformed to phytoclasts, excess SiO<sub>2</sub>, and Ba/Al. They were highly similar with the lower part except some slightly low peaks which could indicate similar high productivity.

The palynological and the geochemical peaks in the lower and upper sections reflect high productivity. One relatively high productivity interval presented in Beds 3 and 27. Both beds showed lower peaks of TOC content which indicated poorer preservation conditions. The upper section of Bed 18 was found to have lower productivity but it showed a high peak of TOC which can also indicate good preservation conditions.

### 5.2 Lacustrine paleoredox condition

In the section that was studied, the high peaks or high concentrations were found to have high paleoredox of the measured section which was similar to the paleoproductivity identified above. Moreover, the ranking of the high values of the relevance may indicate the degree of the paleoredox condition of the section as well.

The lower section showed high values of Beds 5, 8, and 13. The peaks of Beds 5 and 8 corresponded with Ni/Co, U/Th, V/Cr, V/(V+Ni), and (Cu+Mo)/Zn. The peak of Bed 13 supports the conformity in U/Th, V/Cr, and (Cu+Mo)/Zn. All sharp peaks have similar values and patterns which indicated a high degree of reducing condition. Finally, the relatively low peaks of Ni/V indicated a greater reducing condition.

The trends of the upper part fluctuated and showed three high peaks of Beds 17, 20, and 25. The peaks of Beds 17 and 20 were found in the lower parts. They support the

conformity in Ni/Co, V/Cr, V/(V+Ni), and (Cu+Mo)/Zn. The peak of Bed 25 corresponded with Ni/Co, U/Th, V/Cr, and V/(V+Ni). They were high; therefore, they may be used to indicate a high reducing condition. Although the values of Beds 19, 21, and 32 of other proxies were high, the value of Ni/V, which was also still high, can present more oxygenation that affected the benthic floor.

Many high peaks of the paleoredox proxies appeared in the studied section. The high peaks of the V/(V+Ni) and V/Cr values indicated a high redox condition that is mainly under a reducing environment. The studied samples yielded a V/(V+Ni) that ranged from 0.67 to 0.85 which exceeded the cutoff value of 0.46 of a reducing environment. The average value of V/Cr proxy was 2.07 which also exceeded the 2.0 value for an anoxic condition. The lower section (Bed 3) and the upper section (Bed 27) showed higher productivity and lower TOC content which conformed to a lower degree of redox condition. Bed 9 of the lower part showed the highest peak of TOC content which does not reflect excellent preservation due to the potential results from the dominantly high paleoproductivity. Bed 21 of the lower upper section showed lower productivity and the lowest TOC content which indicated a poor reducing effect. Therefore, most of the organic matter is supplied and kept in the benthic floor which fits the association with sediments of black shale. The light grey color of the sediments does not appear in the strata as organic matter in the benthic floor and is not affected by the extreme oxidizing condition.

## 6. Conclusions

AOM, phytoclasts, TOC, excess SiO<sub>2</sub>, Ba/Al, and P/Al are paleoproductivity proxies which have high peaks or high concentrations which can be used to analyze the high productivity of a measured section. The degree of a reducing condition can be assessed by the same productivity method. A high degree of reducing condition or benthic redox condition can be reflected by the high peaks or high values of U/Th, V/Cr, Ni/Co, V/(V+Ni), and (Cu+Mo)/Zn proxies except for Ni/V which is an inverse.

High paleoproductivity presented as high peaks of Beds 3, 9, 12, 14, 20, 16, 17, 22, 27, 30, and 32. Relatively lower paleoproductivity was found in Bed 18 of the upper part but it is high in TOC content. This indicates a high preservation condition which corresponds to high values of the paleoredox proxies. The higher values of V/(V+Ni) and V/Cr which exceeded 2.07 and 2.0, respectively, can indicate an anoxic condition. Moreover, two relatively higher paleoproductivity layers but lower TOC content in Beds 3 and 27 of the lower and the upper parts, respectively, indicate a lower reducing condition.

The Huai Hin Lat shales of the Dat Yai section (Na Pho Song Basin) contain high TOC content (4.7–10.1%) which is all classified as excellent source rocks. They were kept by continuous subsidence since inversion of the Indosinian II Event and continuous subsidence by terrestrial red beds deposit in a large sag basin (Booth & Sattayarak, 2011). Early mature, oil, and some gas were gradually expelled from AOM (belong to only type I kerogen) and some phytoclasts (type III kerogen) to the buttress fold. More mature, whole oil will crack to gas and be kept in proper micropores or structures.

## Acknowledgements

This study was supported by The Commission on Higher Education, Ministry of Education of Thailand and the Royal Golden Jubilee Program of the Thailand Research Fund (RGJ-TRF), the NSFC (project No. 41172202), China Geological Survey Program (No. 1212011121256), and special funding from the State Key Laboratory of Geological Processes and Mineral Resources. Many thanks are conveyed to the officials at the State Key Laboratory of Geological Processes and Mineral Resources and State Key Laboratory of Biology and Environmental Geology, China University of Geosciences, Wuhan.

## References

- Albani, R., Bagnoli, G., Bernárdex, E., Bernárdex, E., Gutiérrez-Marco, J.C., & Ribecai, C. (2006). Late Cambrian acritarchs from the Tuñel Ordovícico del Fabar, Cantabrian Zone, North Spain. *Review of Palaeobotany and Palynology*, 41-52.
- Arsairai, B., Wannakomol, A., Feng, Q., & Chonglakmani, C. (2016). Paleoproductivity and paleoredox condition of the Huai Hin Lat Formation in northeastern Thailand. *Journal of Earth Science*, 3, 350-364.
- Booth, J. & Sattayarak, N. (2011). Subsurface Carboniferous-Cretaceous geology of NE Thailand. In M.F. Ridd, A.J. Barber, & M.J. Crow (Eds.), *The Geology of Thailand* (pp. 185-222). London, England: Geological Society of London.
- Booth, J.E. (1998). The Khorat Plateau of NE Thailand-Exploration history and hydrocarbon potential. *Proceedings of the 1998 SEAPEX Exploration Conference* (pp. 169-202). Singapore.
- Chinoroje, O. & Cole, M. (1995). Permian carbonate in the Dao Ruang-1 exploration well-implication for petroleum potential, Northeast Thailand. *Proceedings of International Conference on Geology, Geotechnology, and Mineral Resources of Indochina* (pp. 563-576), Khon Kaen University, Khon Khaen, Thailand.
- Chonglakmani, C. & Sattayarak, N. (1978). Stratigraphy of the Huai Hin Lat Formation (Upper Triassic) in northeastern, Thailand. *Third Regional Conference on the Geology and Mineral Resources of Southeast Asia* (pp. 739-762), Bangkok, Thailand.
- Chonglakmani, C. (2011). Triassic. In M. F. Ridd, A. J. Barber, & M. J. Crow (Eds.), *The Geology of Thailand* (pp. 137-150). London, England: Geological Society of London.
- D. M. F. (2014). Retrieved from <http://www.dmf.go.th/index.php?act=epsummary&sec=concession>
- D. M. R. (2012). *Huai Hin Lat Stratigraphy; Unpublished report* (63 pp.), Department of Mineral Resources, Bangkok, Thailand.
- Eusterhues, K., Heinrichs, H., & Schneider, J. (2005). Geochemical response on redox fluctuations in Holocene lake sediments, Lake Steisslingen, Southern Germany. *Chemical Geology*, 222, 1-22.
- Haile, N. S. (1973). *GST Newsletter*, pp. 15-16.

- Johnson, C. M., Fawcett, P. J., & Ali, A. S. (2007). Geochemical indicators of redox conditions as a proxy for Mid-Pleistocene climate change from a lacustrine sediment core, Valles Caldera, New Mexico. *New Mexico Geological Society guidebook, 58th Field Conference, Geology of the Jemez Mountains Region II* (pp. 418-423), New Mexico, NM.NM.
- Kobayashi, T. (1973). Upper Triassic estheriids in Thailand and the conchostracan development in Asia in Mesozoic Era. *Geology and Palaeontology of Southeast Asia, 16*, 57-90.
- Martin-Puertas, C., Valero-Garces, B. L., Mata, M. P., Moreno, A., Giralt, S., Martínez-Ruiz, F., & Jiménez-Espejo, F. J. (2011). Geochemical process in a Mediterinian Lake: A high-rezolution study of the last 4,000 years in Zonar Lake, southern Spain. *Journal of Paleolimnol, 46*, 405-421.
- Piyasin, S. (1995). The hydrocarbon potential of the Khorat Plateau. *Proceedings of the International Conference on Geology, Geotechnology and Mineral Resources of Indochina Conference* (pp.551-552), Khon Kaen University, Khon Kaen, Thailand.
- Sattayarak, N., Polachan, S., Assvarittiprom, V., Sitahirun, S., Chaisilboon, B., & Suppitaya, P. (1996). *Field trip guide to sedimentary and petroleum geology marine Permian and non-marine Mesozoic, rim of the Khorat Plateau*. Bangkok, Thailand: Department of Mineral Resources.
- Sattayarak, N., Srikulwong, S., & Pum-In, S. (1989). Petroleum Potential of the Triassic pre-Khorat intermontane basin in Northeastern Thailand. In T. Thanasuthipitak (Ed.), *Proceedings of the International symposium on Intermontane Basins: Geology and Resources Conference* (pp. 43-58), Chiang Mai, Thailand.